Metrol. Meas. Syst., Vol. XXI (2014), No. 2, pp. 305–316.

PAN POLSKA AKADEMIA NAUK

METROLOGY AND MEASUREMENT SYSTEMS

Index 330930, ISSN 0860-8229

www.metrology.pg.gda.pl

M&MS

ULTRASONIC FLOW MEASUREMENT WITH HIGH RESOLUTION

Sławomir Grzelak, Jarosław Czoków, Marcin Kowalski, Marek Zieliński

Department of Technical and Applied Physics, Institute of Physics, Faculty of Physics, Astronomy and Informatics, Nicolaus Copernicus University, Grudziadzka 5, 87-100 Torun, Poland, (✉ slawg@fizyka.umk.pl)

Abstract

The ultrasonic flowmeter which is described in this paper, measures the transit of time of an ultrasonic pulse. This device consists of two ultrasonic transducers and a high resolution time interval measurement module. An ultrasonic transducer emits a characteristic wave packet (transmit mode). When the transducer is in receive mode, a characteristic wave packet is formed and it is connected to the time interval measurement module inputs. The time interval measurement module allows registration of transit time differences of a few pulses in the packet. In practice, during a single measuring cycle a few time-stamps are registered. Moreover, the measurement process is also synchronous and, by applying the statistics, the time interval measurement uncertainty improves even in a single measurement. In this article, besides a detailed discussion on the principle of operation of the ultrasonic flowmeter implemented in the FPGA structure, also the test results are presented and discussed.

Keywords: ultrasonic flowmeter, time to digital converter, programmable logic device, time measurement.

1. Introduction

Ultrasonic flowmeters are a very fast-growing type of flow measurement devices [1, 2]. Although the measurement principle was well known at the end of the XIX century, the first devices appeared in the second half of the XX century. Such devices were used in natural gas flow measurement (linear velocity flow of the order of meters per second) or in district heating water flow measurement (centimetres per second) [3, 4].

In their operation, the following physical phenomena are used: change in the ultrasonic signal transit time at a fixed way, frequency change as the result of reflections from the particles (the Doppler Effect), vortex [5] and surface wave (SAW) modulation [6]. The first two methods are most frequently used for the construction of ultrasonic flowmeters.

A wide-range measurement requires a relatively high-resolution TIMS (Time Interval Measurement System). Usually a high resolution TIMS should be characterized by a resolution better than 1 ns. Such resolution or even better, can be easily achieved in programmable structures [7 – 10]. Implementations of the TIMS in FPGA devices have wide applications from quantum cryptography [11], clock characterization systems [12], experimental physics.

In this paper, a differential and synchronous flow measurement method is presented. At the same time, transducers are excited and pulses in a wave packet are registered. In this way, several time intervals in one measurement cycle are measured. Multiple time interval measurement and application of statistical method of analysis allow to reduce the measurement uncertainty.

Article history: received on Jan. 20, 2013; accepted on Nov. 25, 2013; available online on May. 15, 2014; DOI: 10.2478/mms-2014-0026.

2. Transit time ultrasonic flowmeters

The method of measuring the time difference between the ultrasonic pulses which are propagated in the same direction or in opposite direction to the medium flow is well known. In Figure 1a the flow measurement method is presented.

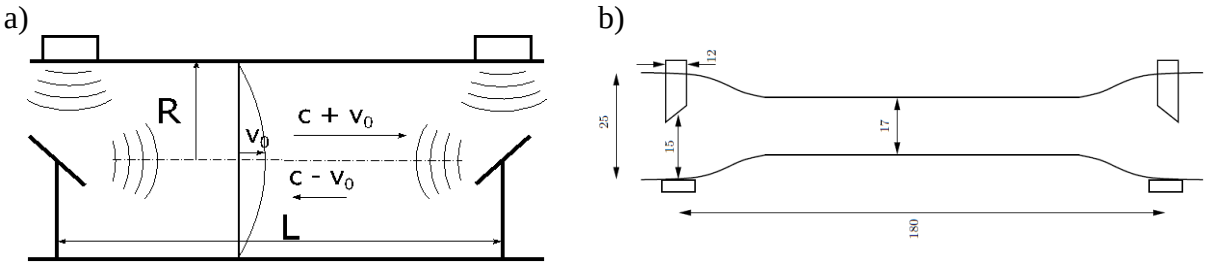

Fig. 1. The ultrasonic flowmeter sensor scheme a), the brass body with dimensions b).

The propagation time in the flow direction can be described as

$$t_1 = \frac{2R}{c} + \frac{L}{c + v_0}. \tag{1}$$

The propagation time in opposition to the flow direction can be expressed as

$$t_2 = \frac{2R}{c} + \frac{L}{c - v_0}. \tag{2}$$

The average flow velocity can be given as

$$v_0 = \frac{L}{2}\left[\frac{\Delta t}{(t_1 - s)(t_2 - s)}\right], \tag{3}$$

where $s = \frac{2R}{c}$, R – the body radius, L is the distance between piezoelectric transducers, c – ultrasonic wave velocity in the medium, Δt – the difference of propagation times. The time difference Δt depends linearly on the flow velocity because the expression in the denominator has a constant value in a given temperature.

To measure small flows about 6 cm/s, a TIMM (Time Interval Measurement Module) with a resolution better than 50 ps must be used, otherwise the "sing around" method can be implemented [13].

The ultrasonic flowmeter sensor consists of stainless steel wave-reflective elements (mirrors) embedded in the brass body. The body is optimized for a low flow (to 400 ml/s) and the mirrors do not disturb the free liquid flow (in this flow range). The sensor is a part of the flow measurement system.

Because a constant flow and simple calibration process must be obtained, a flow measurement system was created (Fig. 2). To ensure a constant height of the water column in the tank, partitions, the overflow vessel at the end of the pipe and a pump whose efficiency is greater than the maximal liquid flow, are used. The volume of flow rate is controlled by one of two valves. A more precise metering valve for flow rates from 0 to 35 ml/s and a less precise second one for flow rates up to 350 ml/s are used. To estimate the liquid flow rate, measurement of mass of the flowing liquid in a given time interval is performed. The flow f is estimated from:

$$f = \frac{m + m_k}{t_m \rho}. \tag{4}$$

where m is the mass of liquid, t_m is the time interval when the solenoid valve is open, m_k is an error correction related to the phenomena such as the time required for stabilization of the flow after the opening of the solenoid valve, and ρ is liquid density. A typical range of t_m in our measurements was from 7 s to 240 s and it depended upon the flow rate. In parallel with the mass of liquid and the time interval, the temperature of liquid in every cycle was also measured.

Actually, for every valve setting, two measurements with different durations are performed: it allows to calculate m_k from the assumption:

$$\frac{m_1 + m_k}{t_{m_1}} = \frac{m_2 + m_k}{t_{m_2}}. \tag{5}$$

Finally, from (4) and (5) we get:

$$f = \frac{(m_1 - m_2)}{\rho(t_{m_1} - t_{m_2})}. \tag{6}$$

Typically we set $t_{m1} = 2t_{m2}$.

It is assumed that measure quantities from (6) are uncorrelated. The standard uncertainty of flow measurement was estimated and it was described as [14]:

$$u_c^2(f) = 2\left(\frac{1}{\rho(t_{m_1} - t_{m_2})}\right)^2 u^2(m) + 2\left(\frac{m_1 - m_2}{\rho(t_{m_1} - t_{m_2})^2}\right)^2 u^2(t_m). \tag{7}$$

In equation (7) $u(m) = 1$ g or $u(m) = 2.4$ g is the standard uncertainty of m measurement for a more precise valve and for a less precise one respectively, and it includes both uncertainties related to accuracy of the scales (0.41 g) and the stochastic character of m measurement (0.81 g and 2.3 g, depending on the used valve) has been accepted. On the basis of more than 200 measurements that standard deviation of m is independent from the duration of measurement and flow rate.

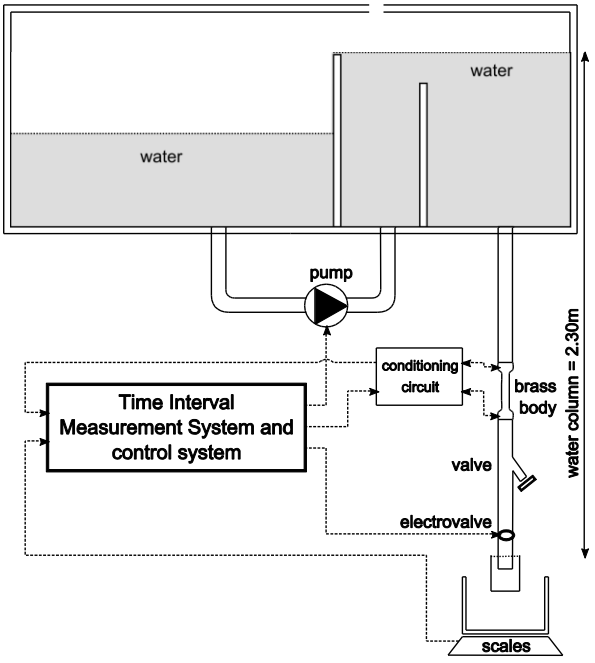

Fig. 2. The liquid flow generation and measurement apparatus.

$u(t)$ is the uncertainty related to stochastic character of opening and closing the solenoid valve and based on the parameters specified by the manufacturer, the valve opening time and the valve closing time is 40 ms, $u(t)$ = 3 ms has been assumed. There is no uncertainty of ρ in equation (7) because its value was described from physical tables and it would have a minor effect on overall uncertainty $u_c(f)$. In such measurements uncertainty $u_c(f)$ for flows below 35 ml/s (more precise valve) and above 35 ml/s (less precise valve) was estimated and it was 0,022 ml/s and 0,6 ml/s respectively. These uncertainties should be included in an uncertainty budget for the flowmeter calibration on this apparatus.

3. Time interval measurement system

The fundamental element of the ultrasonic flowmeter is the time-interval measurement system which consists of the TIMM and the main program which executes the measurement algorithm. The TIMM is implemented in a programmable FPGA Virtex 5 device. A block diagram of the TIMM implemented in the programmable structure is presented in Fig. 3.

The TIMM consists of a tapped delay line with registers, built of four hundred and eighty elements, clock counters, memory blocks, interface and an additional input circuit. Each measured time-interval is the difference between two time stamps. Each time stamp is composed from two parts. The first of them (most important) is taken from the clock counter, while the second (least important) is taken from the tapped delay line register. Usually the tapped delay line is implemented in a single row or column of the configurable logic blocks. The carry chain is used for implementation of the delay elements. Its average resolution of approximately $\bar{q} = 15\,ps$ can be obtained. The characteristic of the TIMM is shown in Fig. 4.

A test density code is used to create this characteristic. The data from the tapped delay line register is collected in memory blocks of the FPGA and it is sent later to the computer after the end of each single measurement cycle.

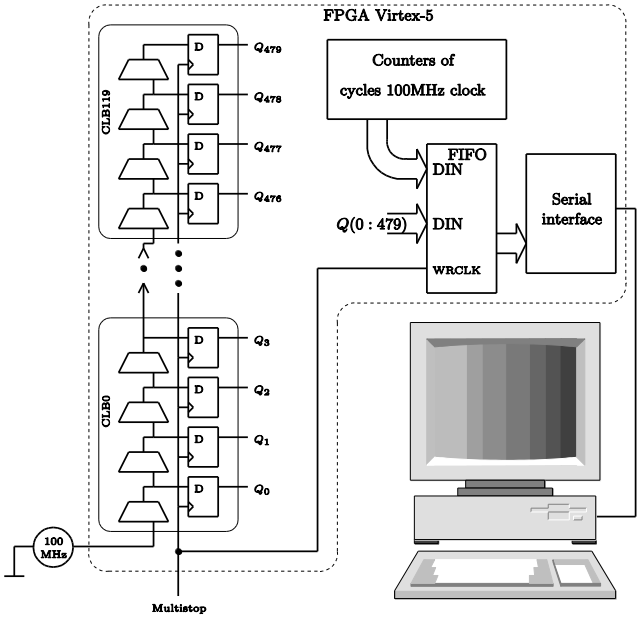

Fig. 3. The block diagram of the TIMM.

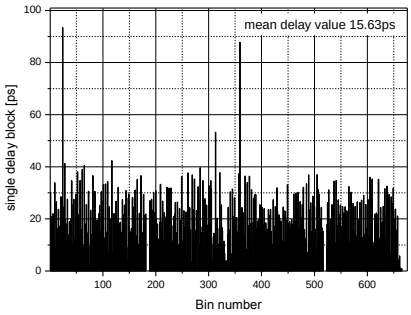

Fig. 4. TIMM module characteristic.

4. Input circuit and time interval measurement method

The input and excitation circuit implemented in FPGA structure is shown in Fig. 5. This part of the ultrasonic flowmeter is used to excite and register the ultrasonic wave. The principle of operation of the ultrasonic flowmeter is presented in Fig. 7.

A single measurement cycle consists of three steps: the excitation process, expectations and register pulses (time-stamps), and the data transfer process (the data is sent to the computer). The measurement starts synchronously with the clock. When the trigger pulse from the TIMM is arriving, then a single excitation pulse as one cycle of a square wave (T = 1 μs, transducers resonance frequency is about 1 MHz) to piezoelectric transducers is generated. After that, two independent packets of ultrasonic waves are being moved by a medium. These packets are registered and formed by the input circuit of the same transducers.

The forming process is shown in Fig. 6. Signals from each of the ultrasonic transducers are fed to the inputs of two comparators. One of them compares the signal with a reference voltage and on this basis the square wave burst Det_L is created. A second comparator forms the square wave burst Det_0 based on zero crossings. Moreover, the first comparator eliminates signal noise and the second allows to determine precise phase pulses in the wave packet.

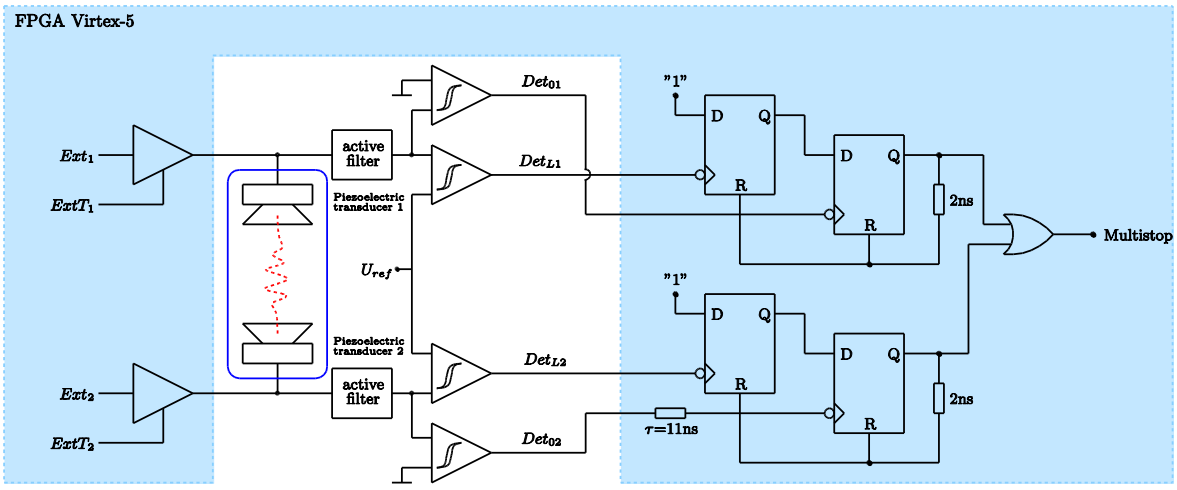

Fig. 5. The input and excitation circuit of piezoelectric transducers.

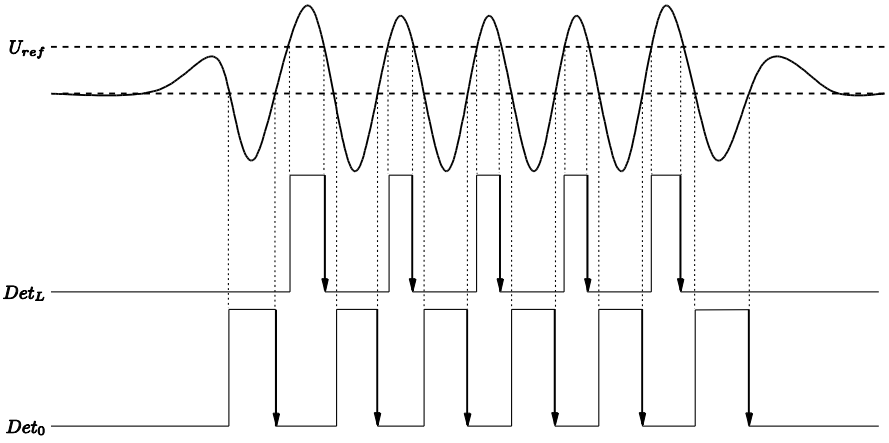

Fig. 6. Pulses shaping for TIMM.

After forming pulses, as it is shown in Fig. 6, both signals are fed to two pairs of the FPGA inputs (Fig. 5 blue area). One of them is delayed by τ = 11 ns but the second is connected directly as presented in Fig. 5. Both signals are connected to the OR gate, and the signal from the output is fed to the input of the measuring module (TIMM).

The TIMS measuring circuit is inactive during the excitation process. The system is enabled to register after a programmably set time. Pulses registered by the TIMM are stored temporarily in a FIFO memory, as shown in Fig. 3. At the next stage, the data is sent to a computer.

The method of the time interval measurement is synchronous and additionally differential. The principle of this method is presented in Fig. 7.

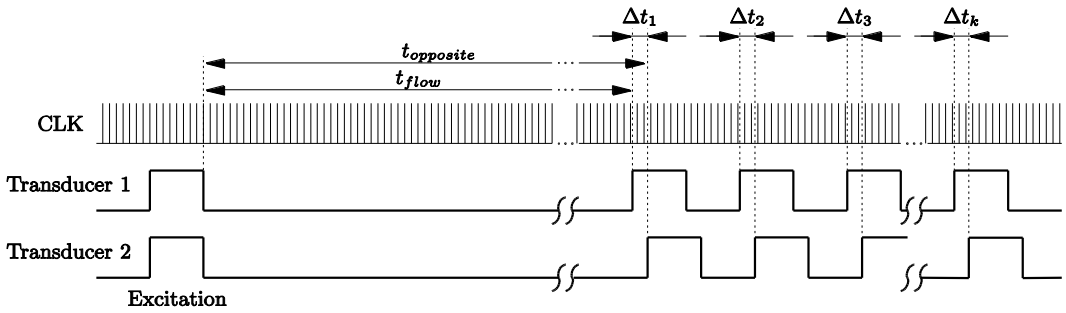

Fig. 7. Principle of operation of the ultrasonic flowmeter.

The single time interval measured by the TIMM can be described as:

$$\Delta t_i = \left(t_{opposite} - t_{flow}\right)_i = \left(m_i - n_i\right)\bar{q}, \tag{8}$$

where m_i, n_i are the numbers of time-bins, $\bar{q}$ is the average width of a time-bin, N number of clock cycles, T_0 clock period, i is the number of pulses in the ultrasonic wave packet.

Generally, the uncertainty in a single time- interval measurement is given as:

$$\sigma_{\Delta t_i} = \sqrt{2\left(\sigma_{INL}^2 + \sigma_q^2 + \sigma_{osc}^2 + \sigma_T^2\right)_i}, \tag{9}$$

where σ_{INL} – is the uncertainty associated with time to digital converter characteristic (integral nonlinearity error), σ_q – quantization effect, σ_{osc} – standard clock uncertainty, σ_T – trigger error.

In the presented system, the excitation signal with the frequency of 1 MHz is created from the main clock signal (100 MHz). In such case, the uncertainty associated with quantization can be written as [15]:

$$\sigma_q = \frac{\bar{q}}{\sqrt{12}}. \tag{10}$$

For the presented system, the uncertainty associated with the quantization effect can be assumed as $\sigma_q = 3{,}5\,ps$.

In this system, time interval measurement is described by equation

$$\Delta t_i = \sum_{i=1}^{m} q_i - \sum_{i=1}^{n} q_i + NT_0, \tag{11}$$

where q_i is a real time-bin width from the density code.

Each of the wave packets consists of several pulses. The time difference between corresponding pulses is similar. In practice, each time interval is measured several times (difference between two single wave packets). In the result, the average time interval obtained during the measurement process (a single time interval measurement) is described by the equation:

$$\overline{\Delta t} = \frac{1}{N}\sum_{i=1}^{N} \Delta t_i, \tag{12}$$

where N – is the number of pulses in the wave packet.
In this way, the uncertainty of a single measurement can be described by the well-known relation:

$$\sigma_{\overline{\Delta t}} = \sqrt{\frac{\sum_{i=1}^{N}\left(\Delta t_i - \overline{\Delta t}\right)^2}{N(N-1)}}, \tag{13}$$

so that in a single measurement cycle the uncertainty decreases as the square root of the number of pulses used.

5. Results of measurements

Undoubtedly, temperature has a significant influence when the ultrasonic wave velocity is measured. This problem is well known, and it was also observed in the system described in this article. Therefore the propagation time measurement at zero flow as a function of temperature of the medium was made. The result of this investigation is shown below (for a body length equal to 18 cm).

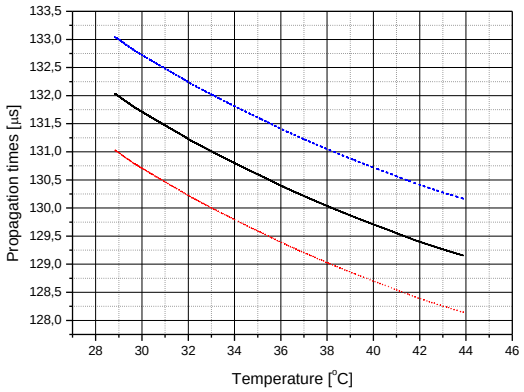

Fig. 8. Propagation time for three pulses in a square wave burst.

If the ultrasonic wave propagation times towards and opposite the flow direction are alternately measured, then changes of temperature have a direct influence on the measured time interval and thereby on the uncertainty of flow measurement. As it is shown in Fig. 8 changes in the temperature of about 0.1°C cause a change of the time propagation on the level of 20 ns.

Therefore, when the propagation time is alternately measured, then the measurement results have large errors.

Another factor which has an impact on the accuracy of the signal propagation time is the type of standard clock oscillator used in TIMM. The results of measurement at zero flow, and the low-stability standard clock oscillator, are presented in Fig. 9.

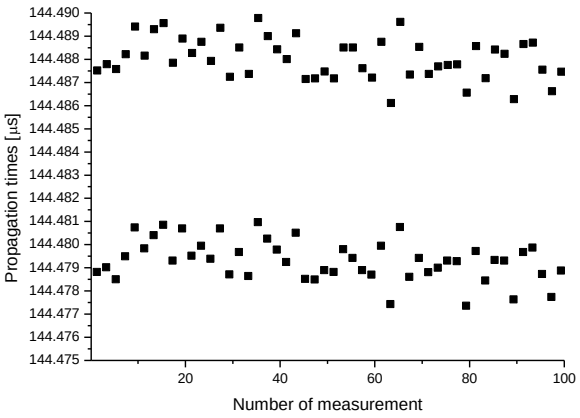

Fig. 9. Signal propagation time towards and opposite the flow direction.

In such experiment the standard clock oscillator EPSON F321G is used. Fig. 9 shows the difference between successive time propagation measurements. The peak to peak value is about 3 ns. In this manner both the temperature and the type of standard clock will affect the flow measurement results of course when ultrasonic wave propagation time is measured alternately.

To reduce the temperature effect, the differential method of propagation time must be applied. In this way, the same contribution is added to propagation time with and against the flow direction. Using the differential method, the temperature influence is reduced. The result of such experiment is shown in Fig. 10.

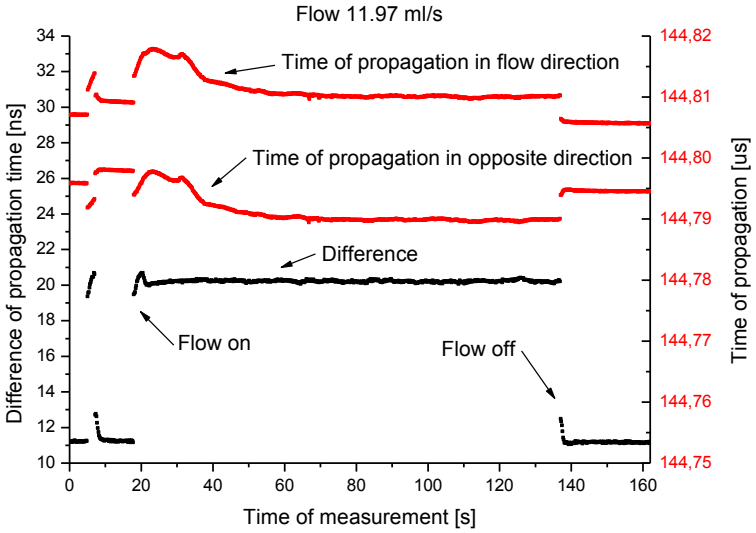

Fig. 10. Propagation times and their difference for flow measurement.

As shown in the figure above, the temperature during the measurement process is changed. So, in Fig. 10 four areas can be distinguished. The first area from 0 s to 20 s is defined. Inside this area, a measurement marker (at 8 s) appeared. Over a period 20 s – 60 s the second area is marked and in this range the flow measurement started (at 20 s). The main source of temperature changes in this case is caused by the sudden flow appearance. The third area is limited from 60 s to 135 s. In this range the temperature is not changed. The last area from 135 s to about 160 s is defined; here zero flow is measured.

Along with temperature changes the propagation time towards and opposite to the flow direction was also changed (red curve in Fig. 10). However, the difference of propagation times is constant (black curve), the spread of the difference of propagation times is approximately 400 ps. In this way, the flow measurement uncertainty will be undoubtedly reduced.

The system implemented in the FPGA structure can register information about a few propagation times in a single measurement. Averaging this information, further reduction of uncertainty is obtained. The results of such research are presented in Fig. 11.

a)

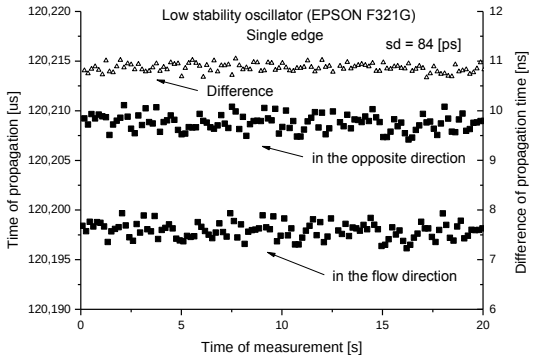

b)

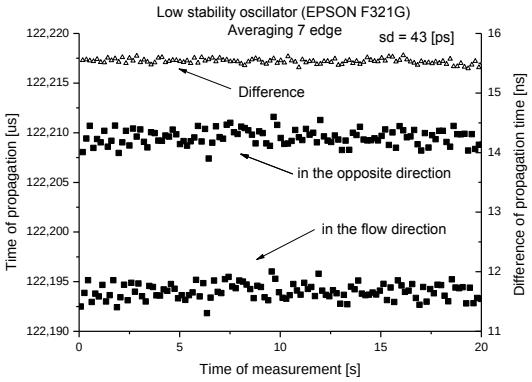

Fig. 11. Propagation times (square points), difference of propagation times (triangle points) as a function of time measurement a) single edge in square wave burst measurement b) averaging 7 edges in square wave burst measurement.

Precision of measurement is associated with spread of results. The spread of measurement can be described by standard deviation. A standard deviation for a single edge in square wave burst measurement equal to 84 ps is obtained. As noted above, some propagation times are registered (in a single measurement cycle). The result is averaged and the standard deviation obtained in measurement process is equal to 43 ps.

When the low-stability oscillator is used (Fig. 9) then the spread of measurement results is large. To reduce the spread of the measurement results, a better clock source was used. For this purpose the oscillator EPSON F321G was replaced by the highly stable oscillator O 100.0-JOB75-3.3-1. Results are presented below.

a) b)

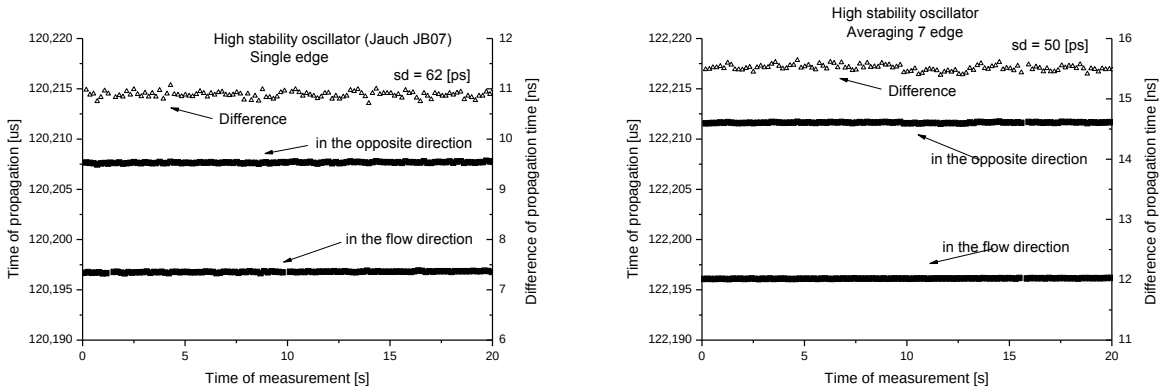

Fig. 12. Propagation times and difference of propagation times as a function of time measurement a) single edge in square wave burst measurement b) averaging 7 edges in square wave burst measurement.

The spread of propagation times obtained in the measurement process (the high-stability oscillator) is more than ten times lower than the spread of propagation times for the low-stability clock oscillator. In this case a spread of propagation times of about 200 ps is measured.

As in the previous case, the standard deviation was reduced by averaging propagation times, here also the same effect was obtained. The standard deviation was reduced from 62 ps to 50 ps and results are presented in Fig.12.

Comparing results of measurement shown in Fig. 11 and Fig. 12, it may be concluded that the high-stability standard clock oscillator is not necessary.

a) b)

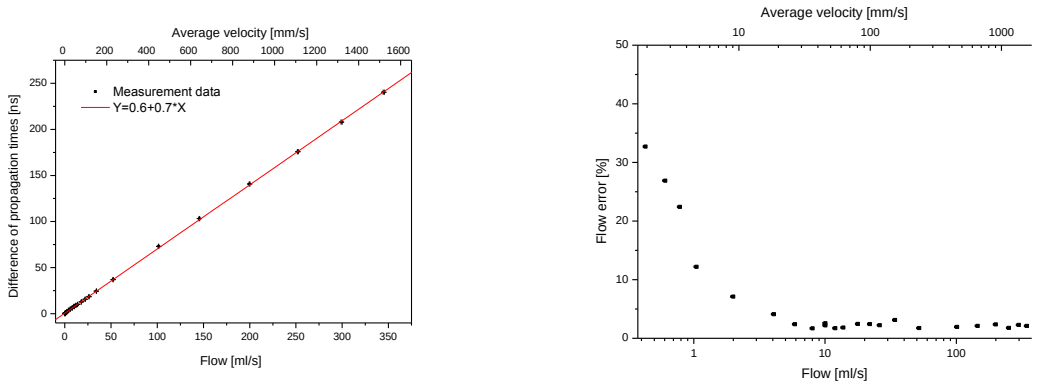

Fig. 13. Flow measurement characteristic in the range from zero flow to 350ml/s a), and its relative error b).

Finally, in Fig. 13, the results of flow measurement are presented, so the ultrasonic flowmeter characteristic and it relative error is obtained. Such a system can measure flows with Reynolds number from 6 to 20000.

6. Summary and Conclusions

Implementation of the TIMM inside the programmable structure [16] allows to decrease the time between projected and finished device. It is known that the hardware is modified during the design process, while the programmable structures can be programmed easily in a complete system without intervention into hardware. Therefore, their use in this type of solutions is justified.

Flow measurement using ultrasonic wave strongly depends on temperature or clock signal stability, as it is shown in this article. It is very important that the propagation time measurement in the same or in the opposite flow direction is measured simultaneously.

Excitation of two piezoelectric transducers at the same time reduced the influence of these factors. Additionally, while propagation times are averaged, the uncertainty of measurement is also reduced and it is shown in Tab. 1.

Tab. 1. The standard deviation of the time interval at constant flow and different measurement modes.

The measurement mode	σ_{t_flow}	$\sigma_{t\_opposite}$	$\sigma_{\Delta t}$
Low stability – single measurement	807 ps	806 ps	84 ps
Low stability - average	788 ps	783 ps	**43 ps**
High stability – single measurement	57 ps	63 ps	62 ps
High stability - average	29 ps	46 ps	51 ps

As it is shown in Tab. 1, the best result was obtained when the low-stability standard clock oscillator and averaging mode were used. This also reduces the quantization error effect by entering the dither signal.

Moreover, if the high-resolution time measurement is used then it allows to measure very small flow. Such a system can measure minimum flow velocity of approximately 0.0008 m/s.

Acknowledgments

This work was supported by the Polish National Science Centre (NCN) Grant No N N505 484540

References

[1] Takamoto, M., Ishikawa, H., Shimizu, K., Monji, H., Matsui, G. (2001). New measurement method for very low liquid flow rates using ultrasound. *Flow Measurement and Instrumentation*, 12, 267–273.

[2] Temperley, N. C., Behnia, M., Collings, A. F. (2000). Flow patterns in an ultrasonic liquid flow meter. *Flow Measurement and Instrumentation*, 11, 11–18.

[3] Baker, R. C.(2005). Flow measurement handbook: industrial designs, operating principles, performance, and applications. *Cambridge Univ. Press*.

[4] Hardy, J. E.,. Hylton, J. O, McKnight, T. E., Remenyik, C. J., Ruppel, F. R.(1999). Flow measurement methods and application. *Wiley - IEEE*

[5] Zhiqiang, S. (2011). Design and performance of the converging-diverging vortex flowmeter. *Metrology and Measurement Systems*, 18(1), 129–136,.

[6] Shrinivas, G. J. (1994). Flow sensors based on surface acoustic waves. *Sensors and Actuators A: Physical*, 44(3), 191–197.

[7] Song, J., An, Q., Liu, S. (2006). A High-Resolution Time-to-Digital Converter Implemented in Field-Programmable-Gate-Arrays. *IEEE Trans. On Nucl. Sci.*, 53(1), 236–241.

[8] Zieliński, M. (2010). Review of single-stage time-interval measurement modules implemented in FPGA devices. *Metrology and Measurement Systems*, 16(4), 641–647.

[9] Zieliński, M., Chaberski, D., Grzelak, S. (2003). Time-interval measuring modules with short deadtime. *Metrology and Measurement Systems*, 10(3), 241–251.

[10] Zieliński, M., Chaberski, D., Kowalski, M., Frankowski, R., Grzelak, S. (2004). High-resolution time-interval measuring system implemented in single FPGA device. *Measurement*, 35(3), 311–317.

[11] Wasilewski, W., Kolenderski, P., Frankowski, R. (2007). Spectral density matrix of a single photon measured. *Phys. Rev. Lett.*, 99(12).

[12] Zieliński, M., Kowalski, M., Frankowski, R., Chaberski, D., Grzelak, S., Wydźgowski, L. (2009). Accumulated jitter measurement of standard clock oscillators. *Metrology and Measurement Systems*, 16(2), 259–266.

[13] Zaworski, Ł., Kowalski, M., Zieliński, M. (2011). Application of FPGA device to ultrasonic flowmeter. *PAK*,12,1151-1514.

[14] Guide to the expression of uncertainty in measurement, International Organization for Standardization, ISBN 92-67-10188-9.

[15] Zaworski, Ł., Chaberski, D., Kowalski, M., Zieliński, M. (2012). Quantization error in time-to-digital converters. *Metrol. Meas. Syst.*, 19(1), 115–122.

[16] Grzelak, S., Kowalski, M., Czoków, J., Zieliński, M. (2014). High resolution time-interval measurement systems applied to flow measurement. Metrol. Meas. Syst., 21(1), 77−84.